scientific reports

Check for updates

OPEN

# Bentonite/Ti(IV) as a natural based nano-catalyst for synthesis of pyrimido[2,1-*b*]benzothiazole under grinding condition

Mina Keihanfar[1], Bi Bi Fatemeh Mirjalili[1]✉ & Abdolhamid Bamoniri[2]

**A new natural-based catalyst named Bentonite/Ti(IV) was prepared and characterized by FT-IR, FESEM, TEM, TGA, EDS-MAP, XRD, BET, XRF, XPS and ICP- MS. An efficient and simple one-pot three-component synthesis of pyrimido[2,1-*b*]benzothiazole derivatives was carried out by the reaction of aldehyde, 2-aminobenzothiazole, and ethyl acetoacetate. In this research, Bentonite/Ti(IV) was used for the synthesis of PBT derivatives in 80 °C under solvent-free conditions by electrical mortar-heater. Solvent-free conditions, simplicity of operation, easy work-up and use of an eco-friendly catalyst are some of advantages of this protocol.**

**Keywords** Natural based catalyst, Pyrimido[2,1-*b*]benzothiazole, Bentonite/Ti(IV)

Recently, the utilization of procedure with high selectivity, low waste production, simple protocol, no usage of column chromatography to purification of products, low cost and high yield of products are advantages of an ideal protocol in organic synthesis[1–5]. Grinding condition for organic synthesis has been attracted increasing consideration[6,7] in the field[8] of green[9–11] chemistry due to the non-use of solvents particularly volatile organic solvents[12]. Grinding methods have other principal advantages such as decrease reaction times[13], high yields[14], increased selectivity[15] and improved safety[16].

Green and sustainable chemistry is one of the key research areas which can pave a way to meet the continuously increasing demand of the population. Nano-catalysis is essential for sustainable and green chemistry[17–30].

One-pot multicomponent reaction has several merits over the routine and step-by-step reaction. Therefore, multicomponent reactions are part of sustainable chemistry and constitute a novel way of ideal organic synthesis. The advantages of one-pot multicomponent reactions are the rapid achievement of complexity and variety in the synthesis of organic materials through highly practical and time-saving approaches. Moreover, this synthetic tool allows chemists to meet the criteria of green chemistry, such as waste prevention, atom and step economy, saving of solvents and reagents, uncomplicated purification procedures, avoidance of hazardous materials, and energy efficiency rather than non-green process[31–38]. Recently, chemists, consider green chemistry law such as choice eco-friendly synthetic methods, solvent-free condition and using nano catalyst. Green chemistry is quickly expanding, offering eco-friendly path- ways significant for sustainable science and industry[39–42].

Currently scientists are trying to minimize the utilization of hazardous chemicals by substituting them with eco-friendly materials. Bentonite is one kind of natural acidic clays with wide availability, low price, large surface area, layered structure and high cation-exchange capability[43].

Bentonite achieve significance in the regard of the researchers as an oncoming catalyst for many organic and inorganic syntheses because of less toxic, high selectivity, high stability, non-corrosive[44–46], and simple work-up[47]. Bentonite has OH groups in its structure that are suitable groups for binding of Lewis acids. In this research, we have reacted bentonite with $TiCl_4$ to production of Bentonite/Ti(IV) as a novel natural based heterogeneous nano-catalyst.

4*H*-pyrimido [2, 1-*b*] benzothiazole derivatives show momentous structural with interesting biological attributes in medicinal and organic chemistry[48–52]. Pyrimidobenzothiazoles show various biological activities such as anti-allergic[53], inhibition of lung cancer[54], anti-tumor[55], anthelmintic[56], antiviral[57], anticonvulsant[58]and antituberculosis[59]. As a consequence, developing environmentally friendly catalytic systems for the synthesis of 4*H*-pyrimido [2, 1-*b*] benzothiazole derivatives is significant. Previously, several methods for the synthesis of pyrimido[2,1-*b*] benzothiazoles using different catalysts such as Nano-Co-[4-chlorophenyl-salicylaldimine-

[1]Department of Chemistry, College of Science, Yazd University, P.O. Box 89195-741, Yazd, Islamic Republic of Iran. [2]Department of Organic Chemistry, Faculty of Chemistry, University of Kashan, Kashan, Islamic Republic of Iran. ✉email: fmirjalili@yazd.ac.ir

pyranopyrimidine dione]$Cl_2$[55], $FeF_3$[60], $Fe_3O_4$@NCs/Sb(V)[61], thiamin hydrochloride (VB1)[62], Camphorsulphonic acid[58], and Nano-$Fe_3O_4$@$SiO_2$–$TiCl_3$[63], have been reported.

The using solvent free condition or green solvents such as $H_2O$ in organic reaction decreases the environmental pollution.

Thus, in this work, we report a simple protocol for the synthesis of 4*H*-pyrimido [2, 1-*b*] benzothiazole in the presence of Bentonite/Ti(IV) via the reaction of 2-aminobenzothiazole, aldehydes and ethyl acetoacetate under grinding and solvent-free conditions at 85 °C (Fig. 1).

## Experimental

### Materials

Chemicals were purchased from Merck, Fluka and Aldrich Chemical Companies. Fourier transform infrared (FT-IR) spectra recorded by ATR method on a Bruker (EQUINOX 55) spectrometer. The electrical mortar-heater was prepared from Borna- Kherad Co., Iran, Yazd. The nuclear magnetic resonance (NMR) spectra were recorded in Acetone and DMSO-$d_6$ on Bruker (DRX-400, Avance) NMR 400 MHz. Melting points were determined by a Büchi B-540 instrument. Field Emission Scanning Electron Microscopy (FESEM) (MIRA 3 TESCAN) and transmission electron microscopy (TEM, CM120) apparatus were used to record of FESEM and TEM images. The XRD graph of catalyst was obtained by X-ray diffractometer (XRD, Bruker -binary V3) using a Cu kα anode (k = 1.54 Å, radiation at 36 kV and 36 mA) in the 2$\theta$ range from 10° to 80°. The X-ray diffraction (XRD Low angle) spectra was obtained by a Philips PW1730 diffractometer equipped with a Cu Kα anode (k = 1.54 Å, radiation at 40 kV and 30 mA) in the 2$\theta$ range from 0.8° to 10°. Energy-dispersive X-ray spectrometer (EDS) and MAP of catalyst were recorded by MIRA II Detector SAMX. Thermal gravimetric analysis (TGA) was done using "BÄHR-(model: STA 504)" instrument. BELSORP MINI II nitrogen adsorption apparatus (Japan) for recording Brunauer–Emmett–Teller (BET) specific surface area of nano-catalyst at 77 K. X-ray Fluorescence (XRF) is an analytical technique that used the interaction of X-rays with a material to determine its elemental composition by Philips PW1730. X-Ray Photoelectron Spectroscopy (XPS) analysis was used to identify the structure of the catalyst by UHV analysis system. All IR, $^1$H NMR and $^{13}$C NMR spectra data are available in ESI (Fig. S1–S33).

### Preparation of Bentonite/Ti(IV)

For the synthesis of Bentonite/Ti(IV), First, in a 25 mL flask, bentonite (0.2 g) and dichloromethane (10 mL) were charged. Then, titanium tetrachloride (2.5 mL) was added dropwise to flask and mixed vigorously for one hour at room temperature. After the completion of the reaction, the resulting suspension was filtered and dried at room temperature (Fig. 1).

### General procedure for the synthesis of pyrimido[2,1-b]benzothiazole derivatives

A mixture of aldehyde (1.0 mmol), 2-aminobenzothiazole (1.0 mmol, 0.15 g), ethyl acetoacetate (1.0 mmol, 0.13 mL) and Bentonite/Ti(IV) (0.06 g) was ground by an electrical mortar-heater at 85 °C. The progress of reaction was monitored by TLC (n-Hexan:EtOAc, 8:2). Finally, 5 mL of hot ethanol was added to the mixture of reaction and the catalyst was separated by filtration. Then, by adding drop-wise water to residue and the product was appeared purely in high yields.

## Results and discussion

### Characterization of Bentonite/Ti(IV)

The structure properties of catalyst were characterized using various techniques, including FT-IR, FESEM, EDX-MAP, XRD, XRF, TGA, XPS and BET. Fourier transform infrared (FT-IR) spectroscopy spectra of Bentonite and Bentonite/Ti(IV) were shown in Fig. 2. In spectrum of Bentonite/Ti(IV), the characteristic absorption band at 787 $cm^{-1}$ (according to previously reported FT-IR about $Ti(OBu)_4$)[55,60] was appeared indicated that $TiCl_4$ have functionalized on Bentonite successfully. The peaks at 3291 $cm^{-1}$ and 1615 $cm^{-1}$ are attributed to the O–H vibrations of water molecules.

Microscopic imaging technique was used to study surface morphology (Fig. 3). These images indicate that Bentonite/Ti(IV) nanoparticles have an average size of less than 40 nm. FESEM (a) Bentonite/Ti(IV), (b) Bentonite and (c) transmission electron microscopy (TEM) of Bentonite/Ti(IV) were investigated for

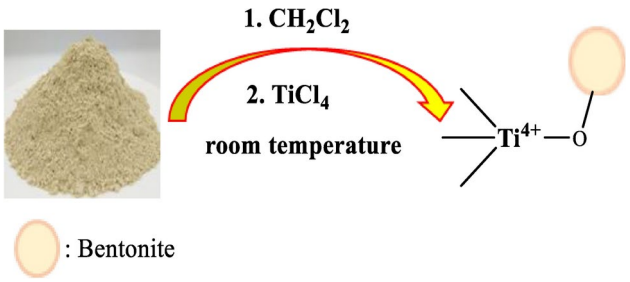


**Fig. 1**. Graphical representation of Bentonite/Ti(IV) synthesis.

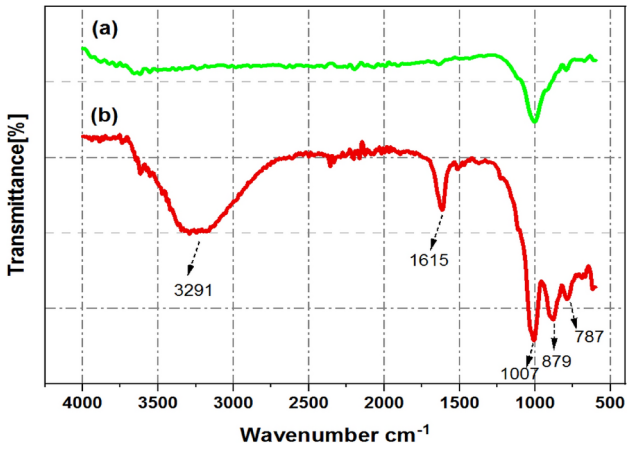


**Fig. 2**. FT-IR spectra of (**a**) Bentonite, (**b**) Bentonite/Ti(IV).

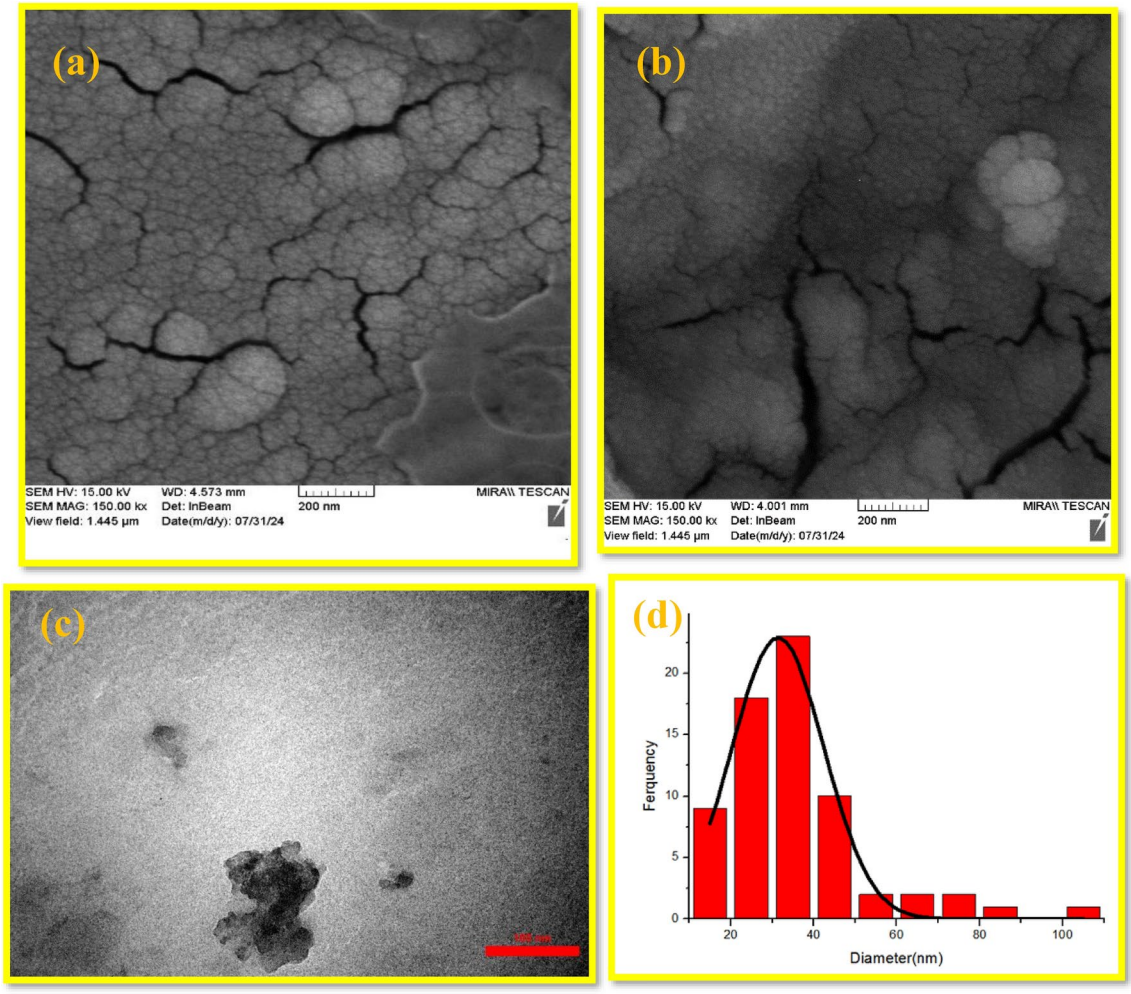


**Fig. 3**. FESEM image of (**a**) Bentonite/Ti(IV), (**b**) Bentonite, (**c**) TEM image Bentonite/Ti(IV) and (**d**) particle size distribution histogram of Bentonite/Ti(IV).

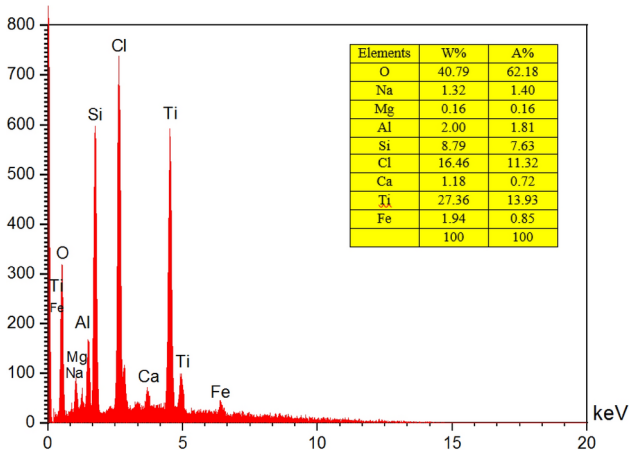


| Elements | W% | A% |
|---|---|---|
| O | 40.79 | 62.18 |
| Na | 1.32 | 1.40 |
| Mg | 0.16 | 0.16 |
| Al | 2.00 | 1.81 |
| Si | 8.79 | 7.63 |
| Cl | 16.46 | 11.32 |
| Ca | 1.18 | 0.72 |
| Ti | 27.36 | 13.93 |
| Fe | 1.94 | 0.85 |
| | 100 | 100 |

**Fig. 4**. EDX analysis of Bentonite/Ti(IV)/

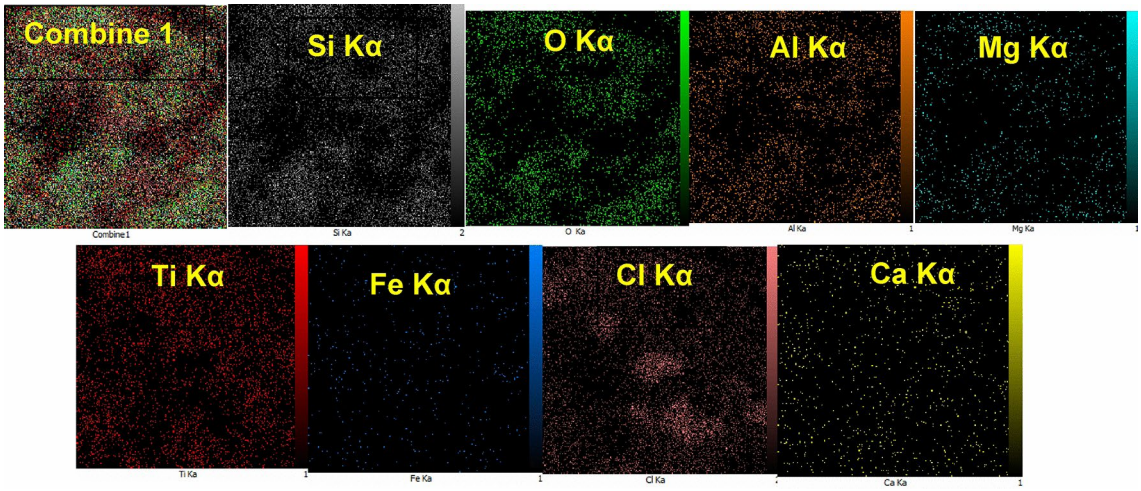


**Fig. 5**. Elemental mapping images of Bentonite/Ti(IV).

determination of their particle size and surface morphology. The histogram of the size distribution was detected by MIRA 3 TESCAN software in FESEM (Fig. 3d).

EDX analysis was applied for the identification of elemental composition in Bentonite/Ti(IV) (Fig. 4). The EDX data confirmed the existence of O, Na, Mg, Al, Si, Cl, Ca, Ti and Fe elements in the catalyst with mass percentages of 40.79, 1.32, 0.16, 2.00, 8.79, 16.46, 1.18, 27.36, 1.94, respectively, and scale bars of 10 µm.

The elemental mapping of Bentonite/Ti(IV) was shown in (Fig. 5) which confirmed homogenous distribution of O, Na, Mg, Al, Si, Cl, Ca, Ti, Fe in catalyst.

The crystalline structure of Bentonite/Ti(IV) was studied by powder X-ray diffraction (Fig. 6). Figure 6a displays sharp peaks at $2\theta = 19.72, 21.92, 23.54, 26.58, 31.67, 50, 62.1$ belonging to Bentonite/Ti(IV). The structure of the catalyst was investigated by X-ray analysis (Low Angle XRD) in the range of 0.8° to 10°, which was used to confirm the mesoporous nature of bentonite (Fig. 6b). The XRD analysis revealed that the pure phase of Bentonite/Ti(IV) has the same pattern as Bentonite, which confirmed the successful catalyst synthesis. Also, we calculated the Miller indices, peak width (FWHM), and particle size of the Bentonite/Ti(IV) were calculated in the range 19.72–62.1. These results can be found in (Table 1). Hence, the particle size (nm) was calculated on the basis of the Debye–Scherrer equation [$D = K\lambda/(\beta\cos\theta)$].

In order to investigate the structure of the Ti(IV)/Bentonite catalyst in more detail, XRF analysis (X-ray fluorescence spectroscopy) was used (Table 2). To determine the thermal resistance of the catalyst, thermal gravimetric analysis (TGA-DTA) was used in the temperature range of 50–600 °C and the weight changes of the catalyst were investigated (Fig. 7). The initial weight loss (endothermic effect at 50–100 °C, 6% weight loss) is related to the removal of moisture. Subsequently, the main weight loss step in the temperature ranges 100–300 °C (60%) is attributed to the loss of coordinated water and decomposition of the clay. respectively., and it cannot be used at a temperature higher than 100 °C.

To distinguish the chemical composition information and oxidation state of the Ti in the Bentonite/Ti(IV) catalyst, X-ray photoelectron spectroscopy (XPS) was conducted in the energy range 0 to 1200 eV (Fig. 8).

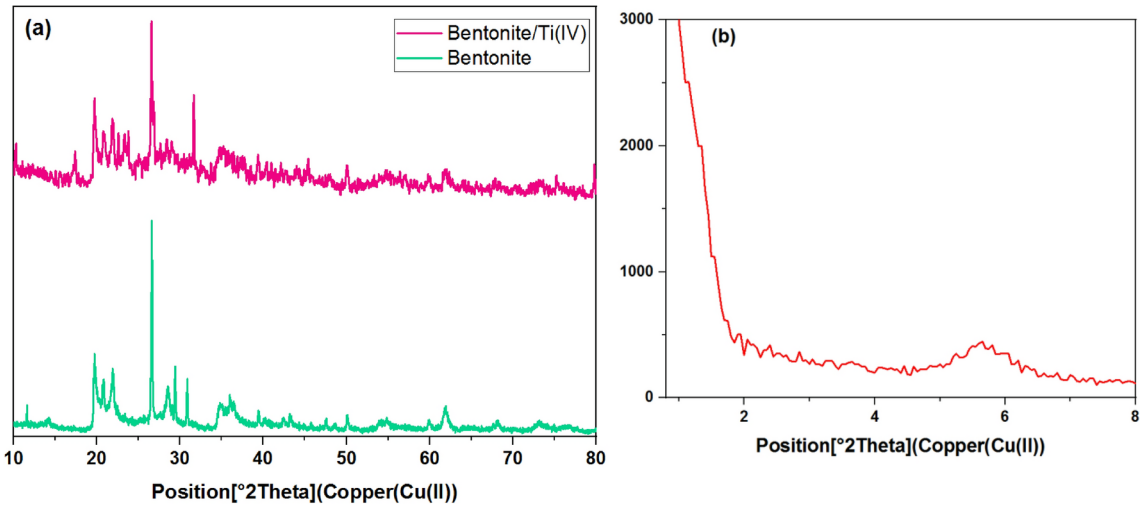


**Fig. 6**. XRD patterns of (**a**) normal, (**b**) Low-Angle.

| Entry | 2θ | Peak width (FWHM) | Miller indices | | | Particle size (nm) |
|---|---|---|---|---|---|---|
| | | | h | k | l | |
| 1 | 19.72 | 0.236 | 0 | 0 | 5 | 35.4 |
| 2 | 21.92 | 0.315 | −1 | 0 | 2 | 26.4 |
| 3 | 23.54 | 0.63 | 0 | 0 | 6 | 13 |
| 4 | 26.58 | 0.118 | 0 | 1 | 1 | 74.2 |
| 5 | 31.67 | 0.118 | 2 | 0 | 0 | 75.1 |
| 6 | 50 | 0.354 | 1 | 1 | −2 | 25.3 |
| 7 | 62.10 | 0.945 | 2 | 2 | 0 | 9.9 |

**Table 1**. The XRD data of Bentonite/Ti(IV).

Figure 8a indicates the survey spectra of the Ti, Si and O elements in Bentonite/Ti(IV). As indicated in the resultant XPS analysis shown in Fig. 8b, the Ti 2p spectrum displayed two peaks with binding energies of around 459.21 and 464.6 eV, which were ascribed to the peaks of $2p_{3/2}$ and $2p_{1/2}$, respectively. The Si 2p XPS spectra in catalyst are also indicated in Fig. 8c. The high-resolution spectra of Si 2p show two peaks at 103.46 and 100.74 eV that were related to Si $2p_{3/2}$ and Si $2p_{1/2}$, respectively. Figure 8d shows the electron binding energies related to O 1 s with three peaks at 533.35, 532.86, 532.18 and 532.1 eV, which are attributed to Si–O, Al–O, Ti–O and O–H, respectively. Furthermore, the peaks observed at 199.7 and 204.7 eV correspond to Cl $2p_{3/2}$ and Cl $2p_{1/2}$, respectively (Fig. 8e).

BET theory was used to measure the porosity and specific surface area of the catalyst. Using the BET diagram, the area of the catalyst was 6.11554 $m^2g^{-1}$ (Fig. 9). Based on the nitrogen absorption and desorption isotherm curve of the catalyst with H3 type hysteresis, the third type isotherm is confirmed to be porous based on the IUPAC and mesoporous classification. According to the results obtained in BJH, the surface area is 8.3399 $m^2\ g^{-1}$, the average pore diameter is 1.21 nm, and the total pore volume is 0.025 $cm^3\ g^{-1}$ (Table 3).

## Investigating the effectivity of Bentonite/Ti(IV) catalyst in the synthesis of 4H-pyrimido[2,1-b] benzothiazole

In order to investigate the performance of Ti(IV)/Bentonite in the synthesis of 4*H*-pyrimido[2,1-*b*] benzothiazole, the reaction of 2-aminobenzothiazole (1 mmol), 4-nitrobenzaldehyde (1 mmol) and ethyl acetoacetate (1 mmol) was considered as the model reaction. In order to optimize the reaction conditions such as temperature, solvent and amount of catalyst, the model reaction was carried out in different conditions of the catalyst. The results of this survey are presented in Table 4. Based on the data in this table, the best conditions for the synthesis of ethyl-2-methyl-4-(4-nitrophenyl)-4*H*-pyrimido[2,1-*b*][1,3]benzothiazole-3-carboxylate in the presence of Ti(IV)/Bentonite (0.06 g) is solvent-free condition at 85 °C. According to the obtained conditions, the desired product is obtained with an efficiency of 96% at 45 min.

According to the obtained optimal conditions, the reaction of different aromatic aldehydes with 2-aminobenzothiazole and ethyl acetoacetate in the presence of 0.06 g of Bentonite/Ti(IV) was done at 85 °C and solvent-free condition, using an electric mortar heater. The obtained results are summarized in (Table 5). Based on the results of Table 5, aldehydes with electron-donating groups show less activity than aldehydes with electron-withdrawing groups.

| Sample. No. | $SiO_2$ | $Al_2O_3$ | $Fe_2O_3$ | CaO | MgO | $Na_2O$ | $K_2O$ | $TiO_2$ | MnO | $P_2O_5$ | LOI |
|---|---|---|---|---|---|---|---|---|---|---|---|
| | % | % | % | % | % | % | % | % | % | % | % |
| T | 34.525 | 6.882 | 2.045 | 1.907 | 1.521 | 1.01 | 0.384 | 20.205 | 0.037 | 0.047 | 21.02 |

| S | Cl | Ba | Co | Cr | Cu | Mo | Ni | Sr | V | Zn | Zr | Ce | La | Pb |
|---|---|---|---|---|---|---|---|---|---|---|---|---|---|---|
| ppm | ppm | ppm | ppm | ppm | ppm | ppm | ppm | ppm | ppm | ppm | ppm | ppm | ppm | ppm |
| 5996 | 103246 | 778 | 42 | 13 | N | N | 22 | 143 | N | N | 93 | 33 | N | N |

**Table 2**. Results of XRF analysis of catalyst.

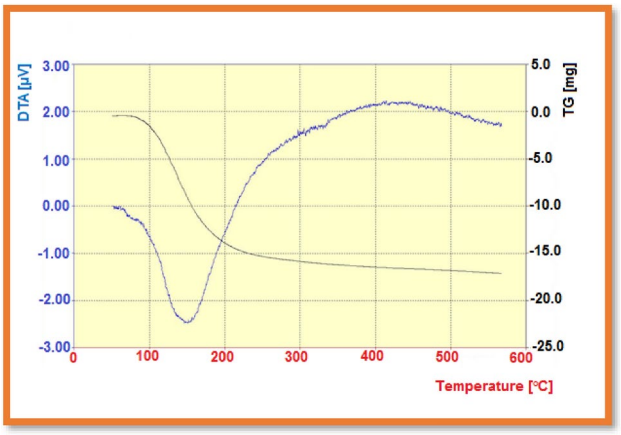


**Fig. 7**. Thermal gravimetric analysis pattern of Bentonite/Ti(IV).

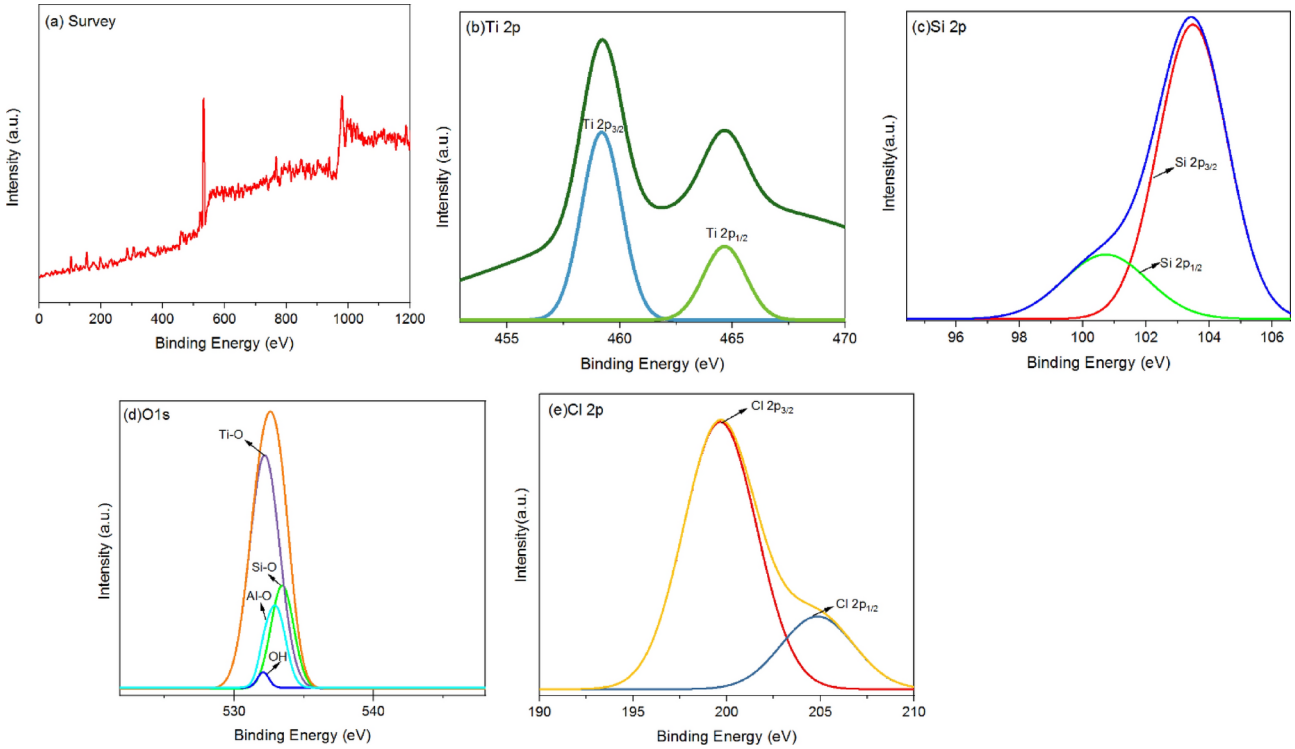


**Fig. 8**. XPS spectra of Bentonite/Ti(IV): (**a**) survey scan, (**b**) Ti 2p, (**c**) Si 2p, (**d**) O1s and (**e**) Cl 2p.

$$\text{TON (turnover number)} = \text{Yield/Amount of Catalyst (mol)}$$
$$\text{TOF (turnover frequency)} = \text{TON/Time (hours)}$$

The Ti in Bentonite/Ti(IV) is the active site of the catalyst. According to ICP data, the amount of Ti in the catalyst is 25%. Here, we have used 0.06 g of catalyst for 1 mmol of substrate. Thus, 0.06 g of catalyst contains $15 \times 10^{-3}$ g of Ti and is equal to $31.3 \times 10^{-5}$ mol of Ti. Thus, the TON and TOF of the catalyst were calculated using the above mentioned data.

The catalytic activity of Bentonite/Ti(IV) in the synthesis of, pyrimido[2,1-*b*]benzothiazole was compared to other reported catalysts (Table 6). According to the data presented in Table 6 displayed excellent catalytic activity with high efficiency in mild conditions. Another advantage of this catalyst is its reusability and cheapness.

The proposed mechanism for the synthesis of 4*H*-pyrimido[2,1-*b*]benzothiazole derivatives is shown in Fig. 10. Initially, the carbonyl group in aldehyde connected to titanium in the catalyst and is activated for condensation. Activated aldehyde and $\beta$-ketoester condense through Knoevenagel reaction to form compound

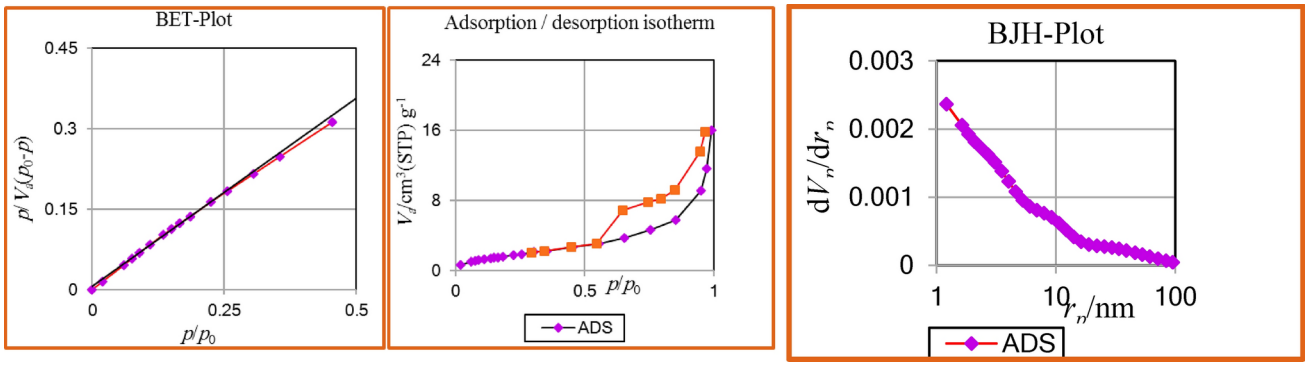


**Fig. 9**. BET plot, Adsorption/desorption isotherm, BJH plot of Bentonite/Ti(IV).

| BET plot | | |
|---|---|---|
| $V_m$ | 1.4142 | [cm³(STP) g⁻¹] |
| $a_{s,BET}$ | 6.1554 | [m² g⁻¹] |
| $C$ | 107.5 | |
| Total pore volume($p/p_0$ = 0.990) | 0.024495 | [cm³ g⁻¹] |
| Mean pore diameter | 15.918 | [nm] |

| BJH plot | | |
|---|---|---|
| **Plot data** | **Adsorption branch** | |
| $V_p$ | 0.025059 | [cm³ g⁻¹] |
| $r_{p,peak}(Area)$ | 1.21 | [nm] |
| $a_p$ | 8.3399 | [m² g⁻¹] |

**Table 3**. Obtained parameters from porosity analysis.

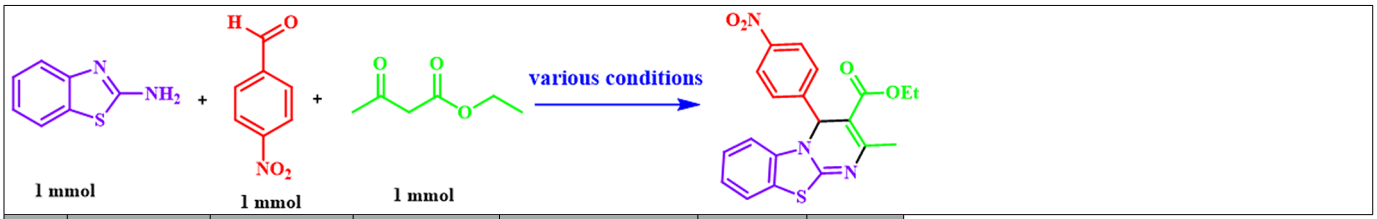


| Entry | Solvent | Conditions (°C) | Catalyst | Amount of Catalyst (g) | Time (min) | Yield (%)[a] |
|---|---|---|---|---|---|---|
| 1 | $H_2O$ | Reflux | Bentonite/Ti(IV) | 0.06 | 200 | 45 |
| 2 | EtOH | Reflux | Bentonite/Ti(IV) | 0.06 | 240 | 55 |
| 3 | $H_2O$/EtOH (1:1) | Reflux | Bentonite/Ti(IV) | 0.06 | 180 | 50 |
| 4 | Solvent-free | r.t | Bentonite/Ti(IV) | 0.06 | 360 | – |
| 5 | Solvent-free | 70 | Bentonite/Ti(IV) | 0.06 | 180 | 80 |
| 6 | Solvent-free | 80 | Bentonite/Ti(IV) | 0.06 | 150 | 71 |
| 7 | Solvent-free | 90 | Bentonite/Ti(IV) | 0.06 | 120 | 87 |
| 8 | Solvent-free | EMH[b]/85 | Bentonite/Ti(IV) | 0.06 | 45 | 96 |
| 9 | Solvent-free | EMH[b]/85 | Bentonite/Ti(IV) | 0.05 | 120 | 75 |
| 10 | Solvent-free | EMH[b]/85 | Bentonite/Ti(IV) | 0.04 | 180 | 60 |
| 11 | Solvent-free | EMH[b]/85 | Bentonite/Ti(IV) | 0.07 | 40 | 73 |
| 12 | Solvent-free | EMH[b]/85 | Bentonite | 0.06 | 45 | 30 |

**Table 4**. The reaction of 4-nitrobenzaldehyde (1 mmol), ethyl acetoacetate (1 mmol) and 2-aminobenzothiazole (1 mmol) under various conditions. [a]Isolated yields. [b]EMH: Electrical Mortar-Heater.

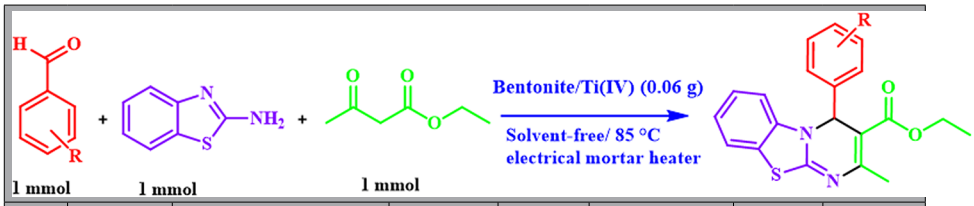


| Entry | R | Product | Time (min) | Yield (%) | TON (TOF, h-1) | M.P. (°C) | References |
|---|---|---|---|---|---|---|---|
| 1 | 4-NO2 | 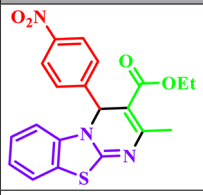 | 45 | 96 | 463(618) | 150–151 | [65] |
| 2 | 4-Cl- | 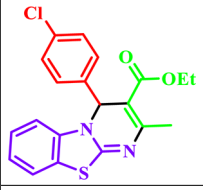 | 40 | 92 | 418(697) | 137–139 | [66] |
| 3 | 4-Br- | 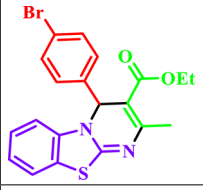 | 50 | 90 | 529(637) | 110 | [66] |
| 4 | 2-Cl | 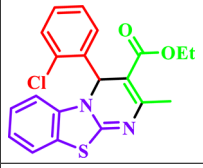 | 45 | 88 | 400(533) | 127–128 | [67] |
| 5 | 3-$NO_2$- | 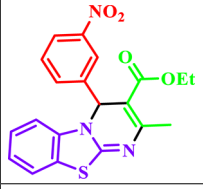 | 70 | 85 | 410(354) | 218–219 | [67] |
| 6 | 2-OEt- | 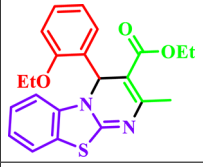 | 80 | 80 | 400(307) | 172–173 | [68] |
| 7 | 4-OH- | 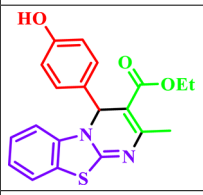 | 75 | 84 | 326(260) | 208–210 | [69] |
| 8 | 2,4$(Cl)_2$- | 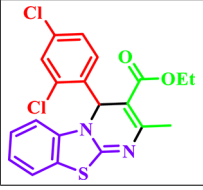 | 120 | 82 | 460(230) | 110–112 | [68] |

Continued

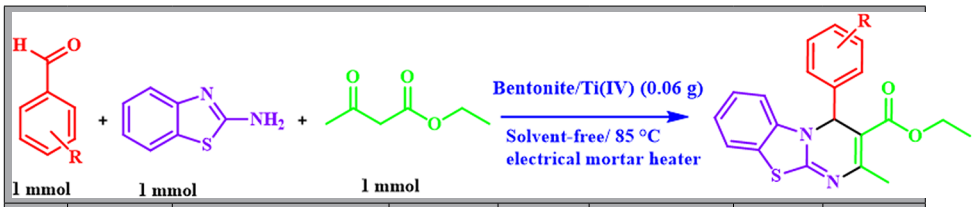


| Entry | R | Product | Time (min) | Yield (%) | TON (TOF, h-1) | M.P. (°C) | References |
|---|---|---|---|---|---|---|---|
| 9 | 2-$NO_2$- | 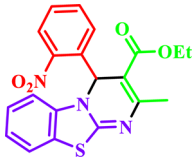 | 50 | 90 | 434(523) | 114–116 | 70 |
| 10 | 3-OH- | 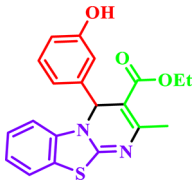 | 90 | 80 | 312(208) | 246–248 | 65 |
| 11 | 2,4-$(OMe)_2$ | 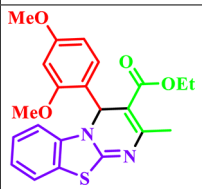 | 110 | 83 | 441(241) | 162–164 | 65 |
| 12 | 3,4-$(OH)_2$ | 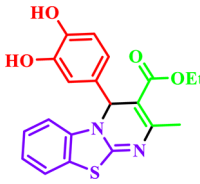 | 85 | 75 | 330(234) | 200 | 65 |

**Table 5**. Synthesis of 4*H*-pyrimido[2,1-*b*]benzothiazole derivatives in the presence of Bentonite/Ti(IV) under solvent- free condition at 85 °C. Reaction conditions: aromatic aldehyde (1 mmol), 2-aminobenzothiazole (1 mmol) and ethyl acetoacetate (1 mmol). [a]Isolated yields.

| Entry | Catalyst | Solvent | Condition (°C) | Time (min) | Yield (%) | References |
|---|---|---|---|---|---|---|
| 1 | Chitosan (0.08 g) | Acetic acid | 65 | 45 | 90 | 63 |
| 2 | Nano-$TiCl_2$/cellulose (0.03 g) | PEG-400 | 70 | 90 | 80 | 64 |
| 3 | Nano-kaolin/$Ti^{4+}$/$Fe_3O_4$ (0.03 g) | Solvent-free | 100 | 90 | 90 | 70 |
| 4 | SMI-$SO_3H$ (0.08 g) | Solvent-free | 100 | 180 | 72 | 71 |
| 5 | nano-$Fe_3O_4$@ $SiO_2$–$TiCl_3$ (0.04 g) | Solvent-free | 100 | 45 | 90 | 65 |
| 6 | (Mg–Al–$CO_3$) (0.05 g) | Solvent-free | 70 | 45 | 79 | 72 |
| 7 | Trypsin (0.03 g) | Ethylene glycol | 60 | 45 | 94 | 73 |
| 8 | Bentonite/Ti(IV) (0.06 g) | Solvent-free | 85 | 45 | 96 | Current work |

**Table 6**. Comparison of Bentonite/Ti(IV) with other reported catalysts in the model reaction.

(I). Then, with the addition of Michael, 2-aminobenzothiazole reacts with compound (I) and iminium ion is formed. Then, by proton transfer and cyclization, the final product is formed by removing water.

In order to study the reusability of the catalyst, after the completion of the model reaction, hot ethanol was added to reaction mixture. The catalyst was separated by filtration, washed with dichloromethane and dried at room temperature. The obtained catalyst was reused in the model reaction under the same conditions and time (45 min) for 5 runs (Fig. 11).

The reused catalyst was analyzed for its chemical properties using XRD and IR techniques. The results revealed no significant structural differences after reusing which indicates the catalyst's chemical stability (Fig. 12).

The weight percentages of Ti(IV) in reused catalyst after five runs was studied by inductively coupled plasma (ICP). According to obtained data, the weight percentage of Ti(IV) is 25%.

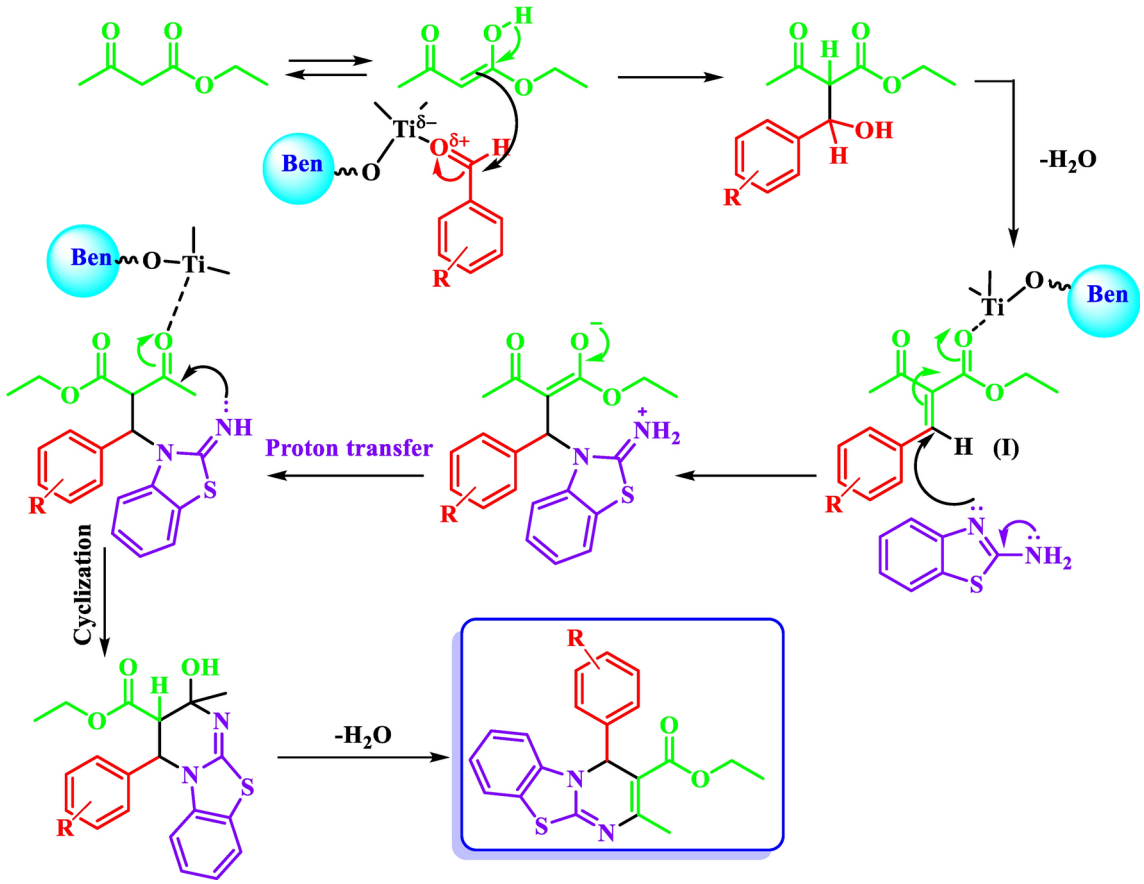


**Fig. 10**. Proposed mechanism for the synthesis of 4*H*-pyrimido[2,1-*b*]benzothiazole derivatives by using Bentonite/Ti(IV)

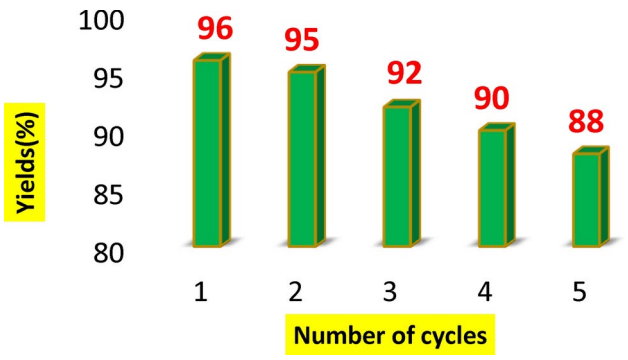


**Fig. 11**. Recoverability of Bentonite/Ti(IV).

## Conclusions

In this study, the Bentonite/Ti(IV) was fabricated as natural-based catalyst to promote the reactions of 4*H*-pyrimido[2,1-*b*]benzothiazole derivatives. This catalyst was confirmed by different techniques as FT-IR, FESEM, TEM, TGA, EDS-MAP, XRD, BET, XRF, XPS and ICP- MS. The results showed that the catalyst Bentonite/Ti(IV) have high catalytic activity, and the reaction products were obtained within 40–120 min. The Bentonite/Ti(IV) displayed excellent catalytic performance in the 4*H*-pyrimido[2,1-*b*]benzothiazole derivatives synthesis and the corresponding products were synthesized in high yields without a difficult work-up procedure. We believe that the modification of the surface of Bentonite by titanium tetrachloride and then using them for the synthesis of heterocyclic compounds such as 4*H*-pyrimido[2,1-*b*]benzothiazole is an effective and practical tool to prepare a suitable catalytic system.

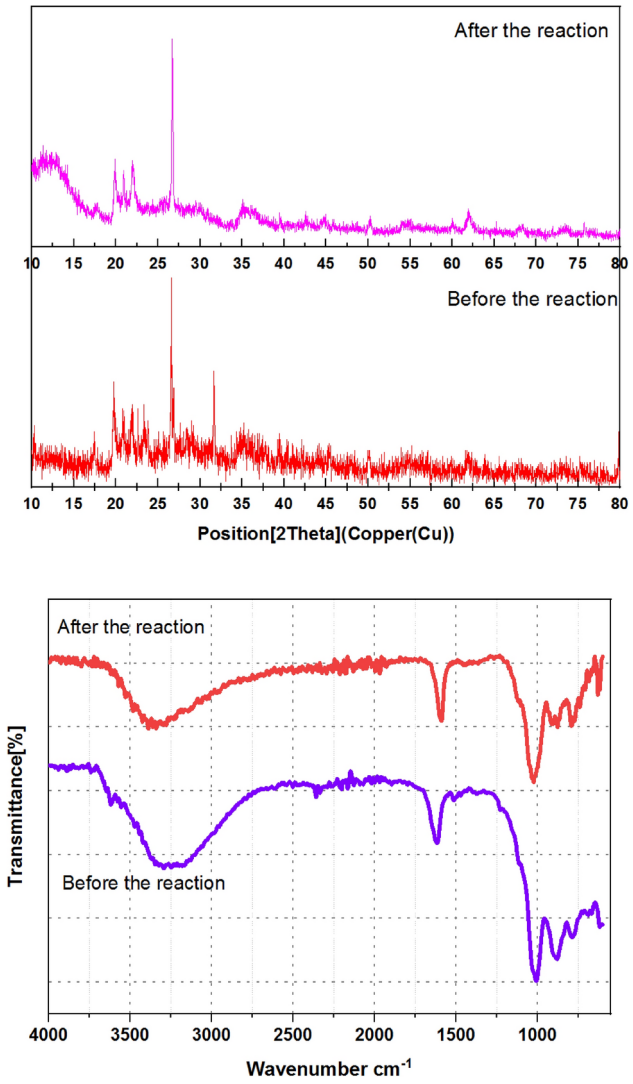


**Fig. 12**. Comparison of the XRD spectra and FTIR analysis of before and after the reaction of the catalyst.

## Data availability

All data generated or analyzed during this study are included in this published article and its supplementary information files.

Received: 30 June 2024; Accepted: 14 November 2024
Published online: 21 February 2025

## References

1. Bhunia, S., Pawar, G. G., Kumar, S. V., Jiang, Y. & Ma, D. Selected copper-based reactions for C– N, C– O, C– S, and C– C bond formation. *Angew. Chem. Int. Ed.* **56**, 16136–16179 (2017).
2. Liu, W., Sahoo, B., Junge, K. & Beller, M. Cobalt complexes as an emerging class of catalysts for homogeneous hydrogenations. *Acc. Chem. Res.* **51**, 1858–1869 (2018).
3. Ai, W., Zhong, R., Liu, X. & Liu, Q. Hydride transfer reactions catalyzed by cobalt complexes. *Chem. Rev.* **119**, 2876–2953 (2018).
4. Ghobakhloo, F., Azarifar, D., Mohammadi, M., Keypour, H. & Zeynali, H. Copper (II) Schiff-base complex modified UiO-66-$NH_2$ (Zr) metal–organic framework catalysts for Knoevenagel condensation–Michael addition–cyclization reactions. *Inorg Chem.* **61**, 4825–4841 (2022).
5. Nikseresht, A., Bagherinia, R., Mohammadi, M. & Mehravar, R. Phosphomolybdic acid hydrate encapsulated in MIL-53 (Fe): A novel heterogeneous heteropoly acid catalyst for ultrasound-assisted regioselective nitration of phenols. *RSC. Adv.* **13**, 674–687 (2023).
6. Maleki, B. et al. Synthesis and characterization of nanorod magnetic Co–Fe mixed oxides and its catalytic behavior towards one-pot synthesis of polysubstituted pyridine derivatives. *Polycycl. Aromat. Comp.* **40**, 633–643 (2018).
7. Salih, A. R. & Al-Messri, Z. A. K. Synthesis of pyranopyrazole and pyranopyrimidine derivatives using magnesium oxide nanoparticles and evaluation as corrosion inhibitors for lubricants. *Eurasian Chem. Commun.* **3**, 533–541 (2021).
8. Baghernejad, B. & Fiuzat, M. A new strategy for the synthesis of 2-amino-4*H*-pyran derivatives in aqueous media using DABCO-CuCl complex as a novel and efficient catalyst. *Eurasian Chem. Commun.* **2**, 1088–1092 (2020).

9. Moosavi-Zare, A. R., Zolfigol, M. A. & Rezanejad, Z. The synthesis of α, α′-bis (arylidene) cycloalkanones using sulfonic acid functionalized pyridinium chloride. *Chem. Methodol.* **4**, 614–622 (2020).
10. Mohamadpour, F. & Feilizadeh, M. Salicylic acid as a bio-based and natural brønsted acid catalyst promoted green and solvent-free synthesis of various xanthene derivatives. *Chem. Methodol.* **4**, 647–659 (2020).
11. Hajinasiri, R. & Rezayati, S. Solvent-free synthesis of 1, 2-disubstituted derivatives of 1, 2-dihydroisoquinoline, 1,2-dihydroquinoline and 1,2-dihydropyridine. *Z. Naturforsch. B.* **68**, 818–822 (2013).
12. Hernandez, J. C. & Bolm, C. Altering product selectivity by mechanochemistry. *J. Org. Chem.* **82**, 4007–4019 (2017).
13. Jameson, L. P. & Dzyuba, S. V. Expeditious, mechanochemical synthesis of bodipy dyes. *Beilstein J. Org. Chem.* **9**, 786–790 (2013).
14. Içli, B. et al. Synthesis of molecular nanostructures by multicomponent condensation reactions in a ball mill. *J. Am. Chem. Soc.* **131**, 3154–3155 (2009).
15. Tan, Y.-J., Zhang, Z., Wang, F.-J., Wu, H.-H. & Li, Q.-H. Mechanochemical milling promoted solvent-free imino Diels-Alder reaction catalyzed by $FeCl_3$: Diastereoselective synthesis of cis-2,4-diphenyl-1, 2, 3, 4-tetrahydroquinolines. *RSC Adv.* **4**, 35635–35638 (2014).
16. Cook, T. L., Walker, J. A. & Mack, J. Scratching the catalytic surface of mechanochemistry: A multi-component CuAAC reaction using a copper reaction vial. *Green Chem.* **15**, 617–619 (2013).
17. Patil, S. M., Tandon, R. & Tandon, N. A current research on silica coated ferrite nanoparticle and their application. *Curr. Res. Green Sustain Chem.* **4**, 100063 (2021).
18. Tandon, R., Tandon, N. & Patil, S. M. Overview on magnetically recyclable ferrite nanoparticles: Synthesis and their applications in coupling and multicomponent reactions. *RSC Adv.* **11**, 29333–29353 (2021).
19. Tandon, N., Patil, S. M., Tandon, R. & Kumar, P. Magnetically recyclable silica-coated ferrite magnetite-$K_{10}$ montmorillonite nanocatalyst and its applications in O, N, and S-acylation reaction under solvent-free conditions. *RSC Adv.* **11**, 21291–21300 (2021).
20. Patil, S. M., Tandon, R. & Tandon, N. Synthesis and characterization of $Fe_3O_4$@ $SiO_2$@ $K_{10}$ NPs applicable for N-tert-butyloxycarbonylation using solvent-free conditions. *J. Phys: Conf. Ser.* **2267**, 012107 (2022).
21. Tandon, R., Patil, S. M., Tandon, N. & Kumar, P. Magnetically recyclable silica-coated magnetite-molybdate nanocatalyst and its applications in N-Formylation reactions under solvent-free conditions. *Lett. Org. Chem.* **19**, 616–626 (2022).
22. Patil, S. M., Ingale, A. P., Pise, A. S. & Bhondave, R. S. novel cobalt-supported silica-coated ferrite nanoparticles applicable for acylation of amine, phenol, and thiols derivatives under solvent-free condition. *ChemistrySelect.* **7**, e202201590 (2022).
23. Patil, S. M. et al. Magnetite-supported montmorillonite ($K_{10}$) (nanocat-Fe-Si-$K_{10}$): An efficient green catalyst for multicomponent synthesis of amidoalkyl naphthol. *RSC Adv.* **13**, 17051–17061 (2023).
24. Patil, S. M., Tandon, R. & Tandon, N. Magnetically recoverable silica-decorated ferromagnetic-nanoceria nanocatalysts and their use with O-and N-butyloxycarbonylation reaction via solvent-free condition. *ACS Omega* **7**(28), 24190–24201. https://doi.org/10.1021/acsomega.2c01107 (2022).
25. Patil, S. M. Novel silica-coated magnetic nanoparticles and their synthetic applications. *Iran. J. Catal.* **13**, 517–523 (2023).
26. Pise, A., Patil, S. M. & Ingale, A. P. Malic acid as a green catalyst for the N-BOC protection under solvent-free condition. *Lett. Org. Chem.* **21**, 620–629 (2024).
27. Patil, S. M. R. & Bedre, A. V. Recent progress in $Fe_3O_4$ nanoparticles and their green applications in organic transformations. *Iran. J. Catal.* **13**, 235–270 (2023).
28. Ingale, A. P., Patil, S. M. & Shinde, S. V. Catalyst-free, efficient and one pot protocol for synthesis of nitriles from aldehydes using glycerol as green solvent. *Tetrahedron lett.* **58**, 4845–4848 (2017).
29. Pise, A. S., Ingale, A. P. & Patil, S. M. An efficient synthesis of 1, 3-oxazine derivatives catalyzed under ceric ammonium nitrate in an aqueous medium at ambient temperature. *Polycycl. Aromat. Comp.* **44**, 5088–5098 (2023).
30. Patil, S. M. et al. One-pot protocol for the reductive amination of aldehydes using thiamine hydrochloride as a green catalyst under solvent-free condition. *Synth. Commun.* **53**, 1545–1558 (2023).
31. Merroun, Y. et al. A Novel heterogeneous catalyst for green synthesis of imidazole derivatives: Environmental sustainability metrics assessment. *Res. Chem. Intermed.* **50**, 3411–3433 (2024).
32. Merroun, Y. et al. Synthesis, characterization, and investigation the catalytic potential of diammonium phosphate modified with bismuth for the one-pot synthesis of 3, 4-dihydropyrimidin-2 (1H)-ones through a three-component reaction: An in-depth evaluation using green metrics. *J. Mol. Struct.* **1306**, 137838 (2024).
33. El Hallaoui, A. et al. Synthesis of new bimetallic phosphate ($Al/Ag_3PO_4$) and study for its catalytic performance in the synthesis of 1,2-dihydro-l-phenyl-3H-naphth [1,2-e]-[1,3] oxazin-3-one derivatives. *Mediterr. J. Chem.* **11**, 215–228 (2021).
34. Chehab, S. et al. A facile and efficient synthesis of tetrahydrobenzo[b]pyrans and dihydropyrano[4,3-b]pyrans derivatives using phosphate fertilizers MAP, DAP, and TSP as heterogeneous catalysts. *J. Iran. Chem. Soc.* **18**, 2665–2678 (2021).
35. Barebita, H. et al. Synthesis and characterization of $Bi13B_{0.48}V_{0.49\text{-}x}P_xO_{21.45}$ and efficient catalyst for the synthesis of 2, 3-dihydroquinazolin-4 (1H)-ones derivatives synthesis. *Bull. Chem. React. Eng. Catal.* **15**, 861–873 (2020).
36. Merroun, Y. et al. Comparative study between the titanium phosphate $TiP_2O_7$ and the phosphate fertilizers in the catalysis of the quinazolin-4 (3H)-one derivatives synthesis. *Mediterr. J. Chem.* **10**, 553–567 (2020).
37. Merroun, Y. et al. Preparation of tin-modified mono-ammonium phosphate fertilizer and its application as heterogeneous catalyst in the benzimidazoles and benzothiazoles synthesis. *React. Kinet. Mech. Catal.* **126**, 249–264 (2019).
38. Chehab, S. et al. Synthesis of 9-arylhexahydroacridine-1,8-diones using phosphate fertilizers as heterogeneous catalysts. *Russ. J. Org. Chem.* **55**, 1380–1386 (2019).
39. Merroun, Y. et al. An effective method to synthesize 2, 3-dihydroquinazolin-4 (1H)-One using phosphate fertilizers (MAP, DAP and TSP) as green heterogeneous catalysts. *J. Turkish Chem. Soc. Sect. Chem.* **5**, 303–316 (2018).
40. Merroun, Y. et al. Triple superphosphate modified by tin (II) chloride: As a reusable and efficient catalyst for the one-pot synthesis of xanthene and xanthenone derivatives under green conditions. *J. Mol. Struct.* **1294**, 136383 (2023).
41. Chehab, S. et al. Catalytic performance of cadmium pyrophosphate in the knoevenagel condensation and one-pot multi-component reaction of chromene derivatives. *J. Chem Sci.* **135**, 95 (2023).
42. Merroun, Y. et al. Synthesis, characterization, and catalytic application of $SnP_2O_7$ for the highly efficient synthesis of xanthene derivatives. *Polycycl. Aromat. Comp.* **44**(3), 1–15 (2023).
43. Dutta, J. & Mishra, A. K. A study on the influence of inorganic salts on the behavior of compacted bentonites. *Appl. Clay Sci.* **116–117**, 85–92 (2015).
44. Wan, D. et al. Adsorption and heterogeneous degradation of rhodamine B on the surface of magnetic bentonite material. *Appl. Surf. Sci.* **349**, 988–996 (2015).
45. Şahin, Ö., Kaya, M. & Saka, C. Plasma-surface modification on bentonite clay to improve the performance of adsorption of methylene blue. *Appl. Clay Sci.* **116–117**, 46–53. https://doi.org/10.1016/j.clay.2015.08.015 (2015).
46. Pusch, R. Use of bentonite for isolation of radioactive waste products. *Clay Miner.* **27**, 353–361 (2018).
47. Ain, Q. U. et al. Facile fabrication of hydroxyapatite-magnetite-bentonite composite for efficient adsorption of Pb (II), Cd (II), and crystal violet from aqueous solution. *J. Clean. Prod.* **247**, 119088 (2020).
48. Atar, A. B., Han, E. & Kang, J. $FeF_3$-mediated tandem annulation: A highly efficient one-pot synthesis of functionalized N-methyl-3-nitro-4*H*-pyrimido [2,1-*b*][1,3] benzothiazole-2-amine derivatives under neat conditions. *Mol. Divers.* **24**, 443–453 (2020).
49. Handique, S. & Sharma, P. Extensive Biginelli reaction: Activated charcoal promoted green approach for one pot synthesis of 4*H*-pyrimido [2,1-*b*][1,3] benzothiazole-3-carboxylate derivatives. *Results Chem.* **5**, 100781 (2023).

50. Merroun, Y. et al. A new heterogeneous catalyst of triple superphosphate/titanium tetrachloride is used for the synthesis of 1, 8-dioxooctahydroxanthenes and tetrahydrobenzo [b] pyrans. *J. Mol. Struct.* **1294**, 136554 (2023).
51. El Hallaoui, A., Merroun, Y., Chehab, S., Ghailane, R. & Souizi, A. One-pot synthesis of 2, 4, 6-triarylpyridines by cyclocondensation between aryl aldehyde, acetophenone derivative, and ammonium acetate using $Al/Ag_3PO_4$ as a new and green bimetallic catalyst. *Monatsh. Chem.* **154**, 231–237 (2023).
52. Chehab, S., Merroun, Y., Ghailane, R., Boukhris, S. & Souizi, A. $Na_2Ca(HPO_4)_2$, an efficient, reusable eco-friendly catalyst for the synthesis of 1, 8-dioxo-octahydroxanthenes and biscoumarin derivatives. *Polycycl. Aromat. Comp.* **43**, 4906–4923 (2023).
53. Yevich, J. P. et al. Antiallergics: 3-(1*H*-tetrazol-5-yl)-4*H*-pyrimido [2,1-*b*] benzothiazol-4-ones. *J. Med. Chem.* **25**, 864–868 (1982).
54. Yadav, M., Deshmukh, V. K. & Chaudhari, S. R. Microwave assisted synthesis and anticancer activity of substituted pyrimido [2,1-*b*] [1,3] benzothiazole derivatives. *Int. J. Pharm. Sci. Rev. Res.* **22**, 41–47 (2013).
55. Moosavi-Zare, A. R., Goudarziafshar, H. & Fashi, P. Nano-Co-[4-chlorophenyl-salicylaldimine-pyranopyrimidine dione] $Cl_2$ as a new Schiff base complex and catalyst for the one-pot synthesis of some 4*H*-pyrimido [2,1-*b*] benzazoles. *Res. Chem. Intermed.* **46**, 5567–5582 (2020).
56. Cai, J. et al. Design and synthesis of novel 4-benzothiazole amino quinazolines Dasatinib derivatives as potential anti-tumor agents. *Eur. J. Med. Chem.* **63**, 702–712 (2013).
57. El-Sherbeny, M. A. Synthesis of certain pyrimido[2,1-*b*]benzothiazole and benzothiazolo[2,3-*b*]quinazoline derivatives for in vitro antitumor and antiviral activities. *vArzneimittelforschung* **50**, 848–853 (2000).
58. Bhoi, M. N., Borad, M. A., Solanki, A. P. & Patel, H. D. Novel 4*H*-pyrimido[2,1-*b*]benzothiazoles derivatives: Camphorsulphonic acid catalyzed enantioselective synthesis, optimization, and biological study. *Phosphorus Sulfur Silicon Relat. Elem.* **198**, 822–835 (2023).
59. Bhoi, M. N., Borad, M. A., Pithawala, E. A. & Patel, H. D. Novel benzothiazole containing 4*H*-pyrimido [2,1-*b*] benzothiazoles derivatives: One pot, solvent-free microwave assisted synthesis and their biological evaluation. *Arab. J. Chem.* **12**, 3799–3813 (2019).
60. Atar, A. B., Jeong, Y. S. & Jeong, Y. T. Iron fluoride: The most efficient catalyst for one-pot synthesis of 4H-pyrimido [2, 1-b] benzothiazoles under solvent-free conditions. *Tetrahedron* **70**, 5207–5213 (2014).
61. Hosseinikhah, S. S. & Mirjalili, B. F. $Fe_3O_4$@ NCs/Sb (V): As a cellulose based nano-catalyst for the synthesis of 4 H-pyrimido [2, 1-b] benzothiazoles. *Aromat. Comp.* **42**, 1013–1022 (2022).
62. Vaidya, S. R. & Chamergore, J. J. Thiamine hydrochloride (VB1) as an efficient catalyst for the synthesis of 4H-pyrimido [2, 1-b] benzothiazole derivatives. *Chem. Biol. Interface* **6**, 47–51 (2016).
63. Sahu, P. K., Sahu, P. K., Gupta, S. K. & Agarwal, D. D. Chitosan: An efficient, reusable, and biodegradable catalyst for green synthesis of heterocycles. *Ind. Eng. Chem. Res.* **53**, 2085–2091 (2014).
64. Azad, S. & Mirjalili, B. F. Nano-$TiCl_2$/cellulose: An eco-friendly bio-based catalyst for one-pot synthesis of 4 H-pyrimido [2,1-*b*] benzothiazole derivatives. *Res. Chem. Intermed.* **43**, 1723–1734 (2017).
65. Fazeli-Attar, S. A. & Mirjalili, B. F. Nano-$Fe_3O_4$@ $SiO_2$–$TiCl_3$ as a novel nano-magnetic catalyst for the synthesis of 4*H*-pyrimido [2,1-*b*] benzothiazoles. *Res. Chem. Intermed.* **44**, 6419–6430 (2018).
66. Khazenipour, K., Moeinpour, F. & Mohseni-Shahri, F. S. Cu (II)-supported graphene quantum dots modified $NiFe_2O_4$: A green and efficient catalyst for the synthesis of 4H-pyrimido [2, 1-b] benzothiazoles in water. *J. Chin. Chem. Soc.* **68**, 121–130 (2021).
67. Safajoo, N., Mirjalili, B. F. & Bamoniri, A. $Fe_3O_4$@ nano-cellulose/Cu (II): A bio-based and magnetically recoverable nano-catalyst for the synthesis of 4 H-pyrimido [2, 1-b] benzothiazole derivatives. *RSC Adv.* **9**, 1278–1283 (2019).
68. Sahu, P. K., Sahu, P. K., Lal, J., Thavaselvam, D. & Agarwal, D. D. A facile green synthesis and in vitro antimicrobial activity 4H-pyrimido [2, 1-b][1, 3] benzothiazole derivatives using aluminum trichloride under solvent free conditions. *Med. Chem. Res.* **21**, 3826–3834 (2012).
69. Shaabani, A., Rahmati, A. & Naderi, S. A novel one-pot three-component reaction: Synthesis of triheterocyclic 4H-pyrimido [2, 1-b] benzazoles ring systems. *Bioorg. Med. Chem. Lett.* **15**, 5553–5557 (2005).
70. Mirjalili, B. F. & Soltani, R. Nano-kaolin/$Ti^{4+}$/$Fe_3O_4$: A magnetic reusable nano-catalyst for the synthesis of pyrimido [2,1-*b*] benzothiazoles. *RSC Adv.* **9**, 18720–18727 (2019).
71. Heravi, M. M. et al. Solvent-free multicomponent reactions using the novel N-sulfonic acid modified poly (styrene-maleic anhydride) as a solid acid catalyst. *J. Mol. Catal. A Chem.* **392**, 173–180 (2014).
72. Mirjalili, B. F. & Aref, F. Nano-cellulose/$BF_3$/$Fe_3O_4$: A magnetic bio-based nano-catalyst for the synthesis of pyrimido [2,1-*b*] benzothiazoles under solvent-free conditions. *Res. Chem. Intermed.* **44**, 4519–4531 (2018).
73. Yu, Y. et al. Enzyme-catalysed one-pot synthesis of 4*H*-pyrimido [2,1-*b*] benzothiazoles and their application in subcellular imaging. *J. Biotechnol.* **324**, 91–98 (2020).


## Acknowledgements

The Research Council of Yazd University gratefully acknowledged for the support for this work.

## Author contributions

M.K., B.F.M. and A.B. designed and performed the research, analyzed the data, interpreted the results, and prepared the manuscript. MK performed the assay and conducted the optimization, and purification of compounds. All authors read and approved the final manuscript.

## Declarations

## Competing interests

The authors declare no competing interests.

## Additional information

**Supplementary Information** The online version contains supplementary material available at https://doi.org/10.1038/s41598-024-80092-z.

**Correspondence** and requests for materials should be addressed to B.B.F.M.